Improved low-frequency sound measurements for impact insulation class (IIC) rating using a comparison technique

Sunit Girdhar[a)] and Andrew Barnard[b)]

(Received: 23 July 2019; Revised: 5 January 2020; Accepted: 6 January 2020)

In multistory buildings, the isolation of sound from floor to ceiling is a major concern. The building codes use an impact insulation class (IIC) rating defined by ASTM to characterize the acoustical performance of floor–ceiling assemblies due to impacts. The measurement process defined in this standard has repeatability and reproducibility limitations due to low-frequency, non-diffuse sound fields in receiving rooms. A comparison method is proposed in this article that uses a reference sample with known sound power to calculate the room or path contribution to the measured sound pressure level, which is then used to calculate the sound power of the floor–ceiling assembly. The proposed method is tested for a small-scale hardboard plate, and the test results are within 1 to 2 dB of baseline sound power values. A simply supported plate used as the reference plate showed MAC values higher than 0.9 for analytical and experimental mode shapes. The analytical natural frequencies are within 1% to 2% of experimental frequencies and analytical sound power values are within 1-2 dB of experimental data. This study showed that for a small-scale assembly, the new method was able to characterize the room contribution within 1 to 2 dB.

Primary subject classification: 51.3; Secondary subject classification: 81.1

1 INTRODUCTION

The growing population and demands of the public are leading to a fast-paced development of multistory residential and mixed-use buildings in cities all over the world. For the safety of the residents, it is important to ensure that the materials and processes used for the construction of the buildings are standardized using building codes. These building codes define some performance requirements for the building, and one of the important requirements is sound isolation between rooms. The sound in a given room may transmit from another room through the walls or windows, or through impacts on the floor–ceiling (FC) assemblies. The efforts for this study are concentrated on the FC assemblies.

Building codes use the impact insulation class (IIC) rating defined by American Society for Testing and Materials (ASTM[1], measurement method similar to ISO 717-2 standard[2]) to characterize the performance of the FC assemblies due to impacts. To measure the IIC rating of an FC assembly, a sample section of the assembly is mounted between a set of two vertically stacked rooms and a standard tapping machine is used to generate an input force in the upper room and on the FC assembly. The sound pressure level (SPL) is measured in the lower receiving room downstairs in one-third octave (OTO) bands ranging from 100 Hz to 3150 Hz[3].

To calculate the IIC rating, a reference contour is defined in the standard (blue curve in Fig. 1), and a constant "T" is added to this curve to match the SPL generated in the receiving room due to the tapping machine input on the FC assembly (example, dashed red curve and solid magenta curve in Fig. 1, respectively) such that the positive difference between the measured response and reference curve is less than 8 dB in any single OTO and the sum of all positive differences is less than 32 dB. The constant T is subtracted from 110 to get the IIC rating.

Several studies in the past have highlighted limitations with the current method[4–10]. For the purposes of this study, the scope is restricted to the non-diffuse measurement issue at low-frequency OTO bands. For smaller test rooms, the low-frequency OTO bands have a non-diffuse acoustic field, meaning that the measured SPL changes based on the microphone location. This results in different IIC values for the same FC assembly when tested in differently sized laboratories, making the IIC test method non-reproducible. The cross-over frequency (f_{co}, in Hz) defines the frequency, above which a diffuse field is observed.

a) Department of Mechanical Engineering — Engineering Mechanics, Michigan Technological University, Houghton, MI 49931, USA; email: sgirdhar@mtu.edu

b) Department of Mechanical Engineering — Engineering Mechanics, Michigan Technological University, Houghton, MI 49931, USA; email: arbarnar@mtu.edu.

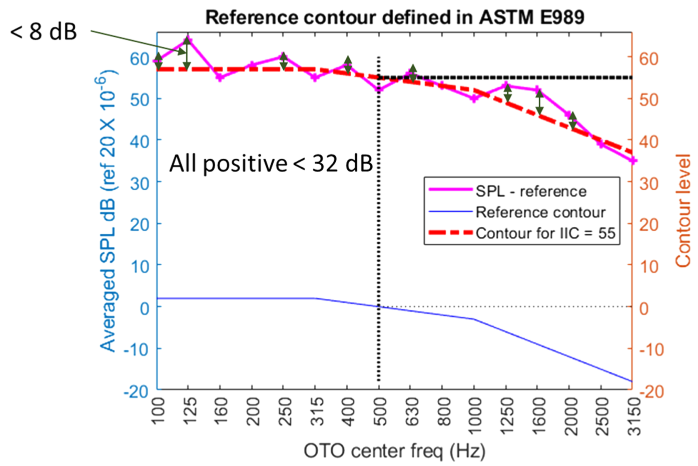

Fig. 1—Example of the IIC rating process for an FC assembly calculated using the reference curve (dashed red curve) and the measured SPL response (solid magenta curve).

It depends upon the volume of the room (V, in m^3) and reverberation time (T_{60}, in seconds) and is defined by Schroeder as:

$$f_{co} = 2000\sqrt{\frac{T_{60}}{V}}. \tag{1}$$

The minimum receiving room requirement for the IIC test is 125 m^3, and a study[11] shows that, for most of the IIC test laboratories in North America, this cross-over frequency lies in the range of 170 to 250 Hz. This indicates that the measurements recorded for frequencies below this for IIC tests are potentially in a non-diffuse field. In the same study, the vibrational response of the FC assembly was measured using accelerometers, and the acoustical response was measured using microphones in the receiving room. For one of the frequencies in the 100 Hz OTO band, the microphone data recorded a peak, but the accelerometer data did not. This means that the high SPL recorded in the microphones for this frequency was due to the acoustic mode in the room and not the FC assembly. This shows that the measurements made in the low-frequency non-diffuse fields are biased because of the contribution of the acoustic room modes[10].

The non-diffuse field problem directly relates to the final IIC rating of an assembly since these low-frequency bands generally control the rating. The measured response of an FC assembly with a bare floor and with different floor coverings is presented in Fig. 2. Note that the data presented is an example of a typical measurement in a certified laboratory and does not represent any particular benchmark. The high deficiencies (vertical bars in Fig. 2) in the 100 Hz OTO band controls the IIC rating and is unaffected with different floor coverings. Therefore, a major limitation of the existing method is the existence of a non-diffuse field for the low-frequency OTO bands that generally control the IIC rating.

The existing method also has a limitation related to the measurement of receiving room absorption using the room decay method described in the standard[1]. For the room decay method, the speakers kept at the corners of the room play a noise signal, and as the signal stops, the reverberation time is measured. These speakers in the corners are not representative of the FC assembly, which is mounted on the top of the room, as viewed from the receiving room, and these different locations excite different acoustic room modes. Additionally, the room decay method gives reliable results only for diffuse fields, and at low frequencies, the field is non-diffuse. The standard dictates a room volume-based frequency range for room absorption measurement, and for the minimum volume of 125 m^3, this range is 400 Hz to 2000 Hz. At OTO bands lower than 400 Hz, the room absorption is not measured.

The problem with the existing method is on a fundamental level. Fundamentally, any noise and vibration problem can be studied in the source–path–receiver domain. For example, if the passengers in a moving car complain about loud noise from the engine, the receivers are the passengers, the source is the engine, and the path is everything in between, including the air, the car chassis, etc. Using this analogy for IIC test for FC assemblies, the source is the assembly itself, the receiver is the measurement microphones, and the path is the receiving room. To truly characterize the performance of FC assemblies, a source quantity should be used, such as sound power (L_w), but the measured SPL for the existing method is a receiver quantity, which depends upon the source and the path. This path (room) contribution creates a bias in the test results, especially in low-frequency non-diffuse fields.

A comparison method (similar to SAE J1400[12] used to test acoustic transmission loss of automotive assemblies and materials) can be used to develop a source-based L_w measurement method, instead of using a source–path-based SPL measurement method. A reference source with known

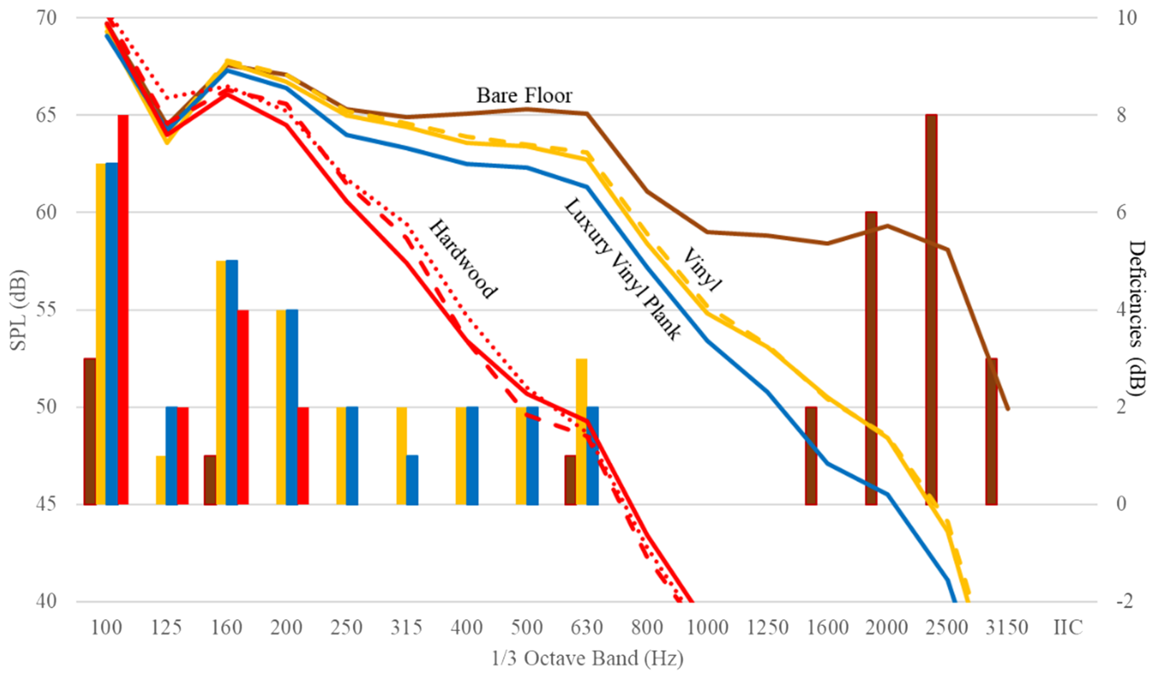

Fig. 2—The measured response of an FC assembly with different floor coverings (lines referenced to the left axes)[11]. Note that the deficiencies in the 100 Hz OTO band (vertical bars referenced to the right axes) control the IIC rating, and this does not change with different floor coverings. Also, note that this figure only plots the bars for positive deficiencies and no positive deficiencies were observed for OTO bands from 800 Hz to 1250 Hz.

sound power (L_w(known)) can be tested in the IIC receiving rooms, and the measured SPL response (L_p(measured, known)) can be used to calculate room contribution or calibration factor (CF) using:

$$L_w(\text{known}) = L_p(\text{measured, known}) + \text{CF}. \quad (2)$$

The L_w of the FC assembly (L_w(unknown)) can be calculated using the measured SPL response (L_p(measured, unknown)) and the known calibration factor (CF) using:

$$L_w(\text{unknown}) = L_p(\text{measured, unknown}) + \text{CF}. \quad (3)$$

The SPL measurements for both the steps are made in the non-diffuse field, so the microphone locations between the two tests should not be changed.

For the comparison method to give reliable results for the FC assembly, it is important to have a reference source with a precisely known sound power level. This could either be calculated analytically or obtained experimentally. For this study, both of these methods were explored. While making analytical predictions, certain assumptions about the material properties and its boundary conditions are required. However, a real test specimen will never precisely match an analytical approximation over the entire frequency range. Therefore, the analytical and experimental results of the reference plate were compared to see the differences. For this study, a simply supported rectangular plate was used as the reference assembly.

2 ANALYTICAL FORMULATIONS

In this section, the formulation for mode shapes, mobility, and sound power radiation of a simply supported rectangular plate are defined.

2.1 Mode Shapes

The analytical mode shapes ($w_{mn}(x,y)$) for a rectangular plate (length l and width b, in m) with simply supported boundary conditions can be calculated for any point (x, y) on the test plate for an integer mode order (m, n, where (m, n) relates to the dimension (l, b) of the plate, respectively) using[13]:

$$w_{mn}(x,y) = \sin\left(\frac{m\pi x}{l}\right)\sin\left(\frac{n\pi y}{b}\right). \quad (4)$$

2.2 Mobility

The mobility (mob) of a response location (x_r, y_r) for an input force (F, in N) at an input location (x_f, y_f) for radial frequency (ω, in rad/sec) at a single modal frequency (ω_{mn}) is given by[13]

$$\begin{aligned}\text{mob} &= \frac{v(x_r,y_r)}{F(x_f,y_f)}(\omega)\\ &= \sum_{m=1}^{\infty}\sum_{n=1}^{\infty}\frac{\iota\omega}{MM}\frac{A_{mn}(x_r,y_r,x_f,y_f)}{\omega_{mn}^2-\omega^2},\end{aligned} \quad (5)$$

where the modal mass (MM) for a plate of thickness (h, in m) and density (ρ, in kg/m^3) is given by:

$$\mathrm{MM} = \frac{lbh\rho}{4}, \tag{6}$$

and modal coefficients (A_{mn}) are given by:

$$A_{mn}\left(x_r, y_r, x_f, y_f\right) = \left[\left(\sin\left(m\pi\frac{x_r}{l}\right)\sin\left(n\pi\frac{y_r}{b}\right)\right)\left(\sin\left(m\pi\frac{x_f}{l}\right)\sin\left(n\pi\frac{y_f}{b}\right)\right)\right]. \tag{7}$$

The loss factor of a test plate plays an important role in mobility calculations but is challenging to predict analytically. For this study, the loss factor was obtained experimentally from the actual assembly using a time domain decay method and averaged over all the modes in the bandwidth.

As a sanity check on the analytical calculations, the response of an infinite plate (mob_{inf}) was computed. This response is a straight line over the entire frequency bandwidth and should approximately be the mean response of the test panel. This is given by[13]

$$\mathrm{mob}_{inf} = \frac{1}{8\sqrt{D\rho h}}, \tag{8}$$

where flexural rigidity (D) depends upon Young's modulus (E, in Pa), Poisson's ratio (υ), and thickness of the plate and is given as:

$$D = \frac{Eh^3}{12(1-\upsilon^2)}. \tag{9}$$

2.3 Sound Power Radiation

The sound power radiation of a simply supported rectangular plate for a spherical coordinate system (r, θ, φ) is widely studied[13–16]. Sound power (P, in W) for 1/8th of a sphere (quadrant) is given by 10:

$$P = 8\rho_0 c_0\left(\frac{u_m k_0 lb}{\pi^3 mn}\right)^2 \int_0^{\frac{\pi}{2}}\int_0^{\frac{\pi}{2}} \left\{\frac{\begin{matrix}\sin\\ \cos\end{matrix}\left(\frac{\alpha}{2}\right)\ \begin{matrix}\sin\\ \cos\end{matrix}\left(\frac{\beta}{2}\right)}{\left[(\alpha/m\pi)^2-1\right]\left[(\beta/m\pi)^2-1\right]}\right\}^2 \sin\theta d\theta d\varphi, \tag{10}$$

where sin is used for even values of (m, n) and cos is used for odd values of (m, n) in the numerator, ρ_0 is the density of air (kg/m^3), c_0 is the speed of sound in air (m/s), k_0 is the wavenumber in air (m^{-1}), α, β are given as:

$$\alpha = k_0 l \sin\theta \cos\varphi, \text{ and} \tag{11}$$

$$\beta = k_0 b \sin\theta \sin\varphi, \tag{12}$$

and u_m depends on the surface averaged normal velocity of the plate ($\langle u_w\rangle^2$), given by

$$\frac{u_m^2}{8} = \langle u_w\rangle^2 = \frac{1}{lb}\int_0^l\int_0^b \frac{1}{2}u_w^2 dxdy. \tag{13}$$

The experimental sound power was obtained using a discrete point intensity test using a p-p type intensity probe, where the power is given by intensity multiplied by the measurement area. The sound pressure data recorded in the two microphones were converted to intensity ($I(\omega)$ in W/m^2) using the imaginary part of the cross-spectrum of the microphones (imag(G_{12})) and microphone spacing (Δr in m) and is given by[17]

$$I(\omega) = \frac{\mathrm{imag}(G_{12})}{\omega\rho_o\Delta r} \tag{14}$$

3 VALIDATION OF THE PROPOSED METHOD

The proposed comparison technique for IIC tests was validated in three stages: construction of the reference assembly, a study of the reference assembly—analytically and experimentally, and proof of concept using a new, unknown assembly.

3.1 Construction of the Reference Assembly

The reference assembly was constructed from a 30 in × 19 in × 0.125 in (762 mm × 482.6 mm × 3.18 mm) ABS plastic panel (material properties are shown in Table 1). The test plate was mounted with simply supported (SS) boundary conditions on all four sides. This SS assembly was built based on a previous work[18] where the authors glued thin aluminum side "blades" to the aluminum test plate and bolted this assembly to a heavy, rigid aluminum base. The authors observed less than 4% error between the first ten analytical and experimental natural frequencies with the consideration of the weight of the base frame to be at least ten times more than the test structure. This design concept was used to build the assembly for this work by using thin ABS plastic side blades and a heavy, rigid gypsum concrete base where the weight requirements were met.

Table 1—Material properties for ABS plastic panel used as the reference assembly.

Material property	Value
Young's modulus	2.25×10^9 Pa
Density	1030 kg/m^3
Poisson's ratio	0.35
Loss factor	0.0137

The physical assembly was built in three steps shown in Fig. 3. Steps 1a and 2a show the gypsum mold used as the base frame, and steps 1b and 2b show the test plate and the glued side blades, respectively. This assembly was then pushed into the gypsum mold and left to dry for one week. Once dried, the side wooden frame members were removed.

The Young's modulus, Poisson's ratio, and density of the ABS plastic material were tested using the samples cut from the scrap material. The analytical natural frequencies computed using these values of Young's modulus and Poisson's ratio (1.88×10^9 Pa and 0.41, respectively) were approximately 6.5% lower than the experimental values on an average. The Young's modulus and Poisson's ratio values were modified by 19.6% and 14.6%, respectively, to the values shown in Table 1 to improve the comparison of analytical and experimental data. It is believed that this error was caused by the additional edge stiffness induced by the plastic blades glued on the side for SS boundary conditions. The plate was not perfectly flush with the tops of the plastic blades, which could result in added edge stiffness. The density values obtained from the test were kept unchanged and are shown in Table 1.

The reference test plate shows good reciprocity at frequencies below 500 Hz (Fig. 4). This shows that the structure is linear in this frequency bandwidth. The details of the points used for Fig. 4 (points 124, 101, and 190) are provided in the upcoming sections.

3.2 Study of the Reference Assembly

The comparison method is only as good as the known sound power of the reference assembly. Therefore, a lot of effort in this study was spent on understanding the ABS plastic reference assembly. In this section, the mode shapes, mobility, and sound power radiation of the reference test plate are discussed.

3.2.1 Mode shapes

A roving hammer experimental modal analysis was performed on 247 grid points (Fig. 5, left), 19 on the longer side and 13 on the shorter side, and the response was recorded at four locations (Fig. 5, right). The input force was provided using a PCB modal impact hammer (086C03), and the response was recorded using PCB uniaxial accelerometers (352A21). The data acquisition parameters are mentioned in Table 2.

The ABS plastic test plate was highly responsive, and double hits were observed for the hard steel tip and the medium vinyl tip for the modal hammer[19]. The structure was excited with a super soft tip to avoid double hits. This resulted in a usable bandwidth up to 500 Hz. The data was measured with seven averages for each location, and the FRFs showed good overlap for averages ranging from three to seven[19].

The results in this section are presented for frequencies ranging from 100 Hz to 500 Hz with an extra attention to the 250 Hz OTO band. This OTO band is well excited by the modal hammer, and the plate had eight modes. The poles and residues of all the modes were solved using the Polymax algorithm available in the Testlab software,

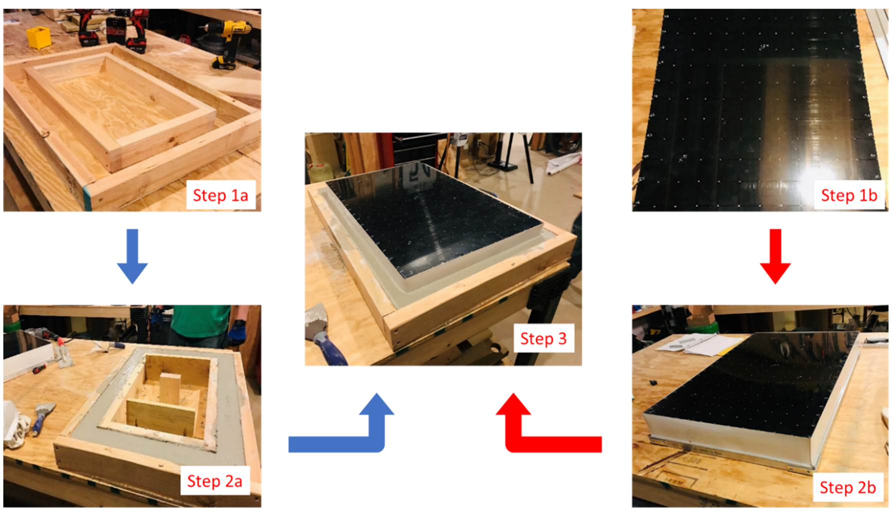

Fig. 3—The reference test assembly was built in three steps using gypsum mold (step 2a), test plate (step 1b), and side blades (step 2b). After step 3, the assembly rested until dry.

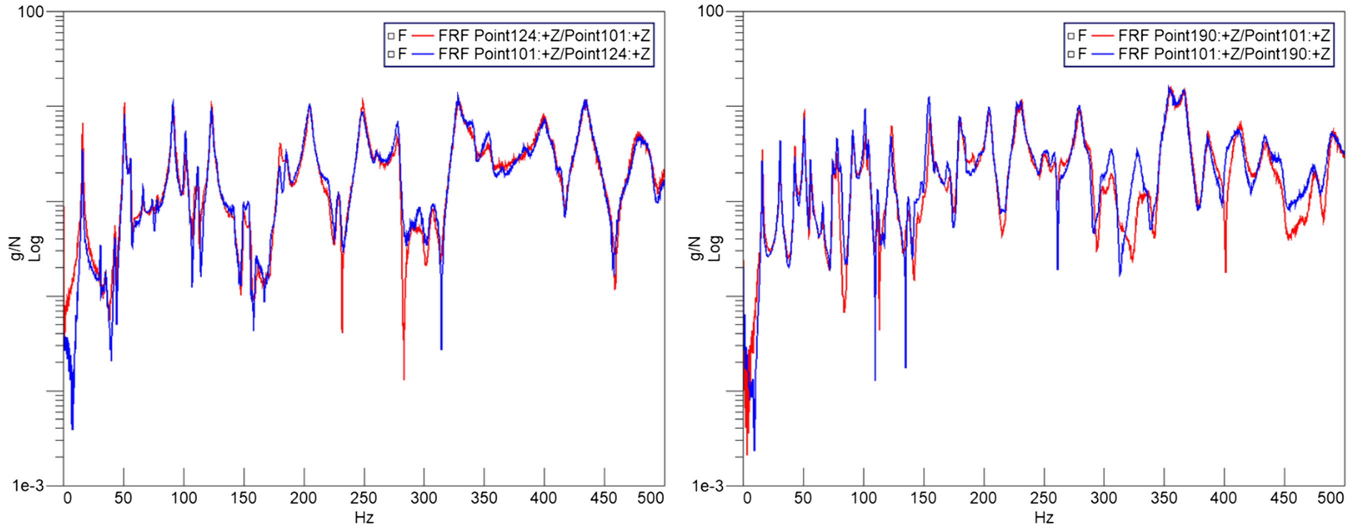

Fig. 4—Good reciprocity observed at frequencies below 500 Hz for two sets of points on the reference test plate.

and a screenshot for solution of 250 Hz OTO band is shown in Fig. 6. Based on the analytical predictions, eight stable modes highlighted with red were expected, but one stable mode (~232 Hz) highlighted with blue was not. This mode may be a mode of the concrete base frame.

To show this, a modal analysis was performed on the concrete base frame on 20 points with the same acquisition parameters as shown in Table 2, and a concrete mode was observed at ~232 Hz (shown in Fig. 7). The concrete base is affecting the response of the test plate in the frequency bandwidth of interest. The consideration of the weight of the base frame to be at least ten times heavier[18] than the test plate is not enough to ensure that the test plate response is unaffected.

The analytical and experimental mode shapes for the reference test plate correlate well with each other (Fig. 8 and Appendix A). MAC values computed for experimental and analytical data are close to one. MAC comparison for analytical and experimental data for plate modes till 500 Hz OTO shows good correlation with the diagonal values for the MAC matrix close to one, shown in Fig. 9.

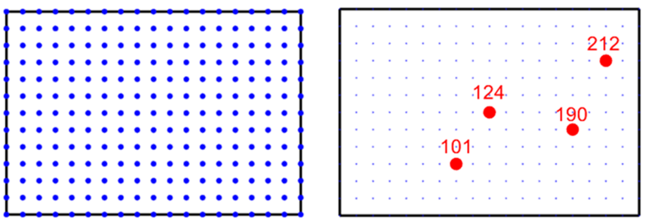

Fig. 5—A total of 247 grid points used for modal analysis shown on the left and four response locations shown on the right.

3.2.2 Mobility

The mobility of the reference test plate was calculated by dividing the accelerance (recorded by the accelerometers used for the modal analysis) by $\iota\omega$. The analytical and experimental driving point mobility response shows good comparison, and the analytical natural frequencies are within 1% to 2% of experimental frequencies, averaged till 500 Hz for all four response locations[19]. This comparison is presented in Fig. 10. The analytical predictions (An.) are shown with a dotted blue line, experimental predictions (Exp.) are shown with a solid red line and the infinite plate response (Inf.) is represented with a solid black line. For better understanding, Fig. 11 shows the comparison of the analytical and experimental mobility for 250 Hz OTO. Overall, the analytical and experimental mobilities compare well till 500 Hz, and the infinite plate response is approximately the mean of the test plate's response.

The surface averaged mobilities for the test plate till 500 Hz are presented in Fig. 12. Same curve color scheme is followed as Fig. 10, and the natural frequencies predicted analytically are within 1% to 2% of experimental data. For clarity, the mobility comparison for 250 Hz OTO

Table 2—Data acquisition parameters for the experimental modal analysis.

Parameter	Value
Software used	Simcenter Testlab spectral testing
Frequency resolution (Δf)	0.25 Hz
Acquisition time	4 s
Bandwidth	1024 Hz
Window on the channels	Uniform

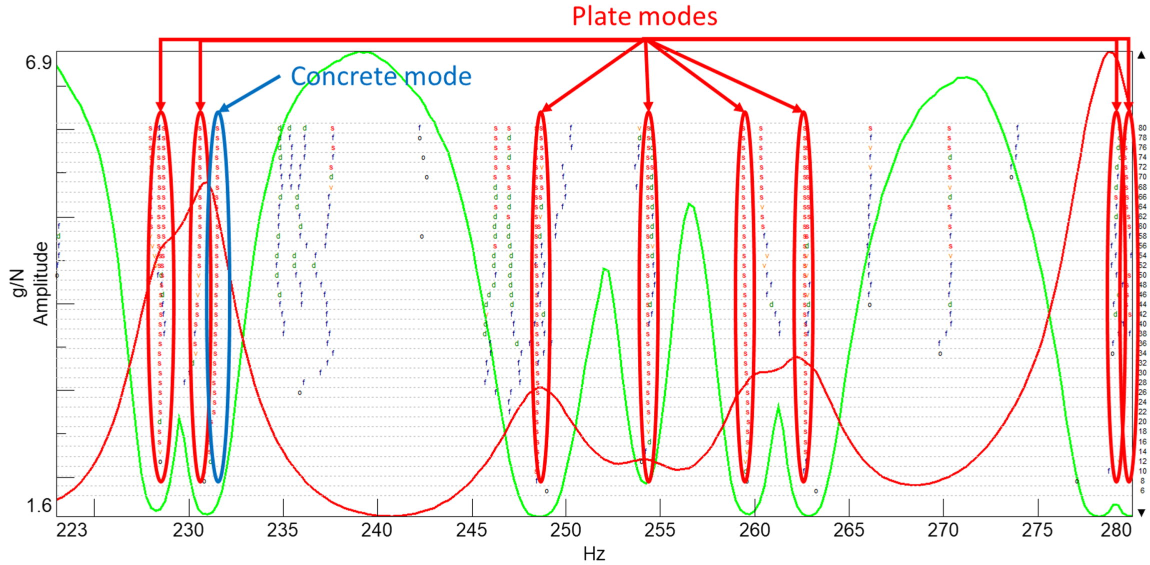

Fig. 6—Stabilization diagram for 250 Hz OTO shows the eight plate mode and one mode of the concrete base frame.

band is presented in Fig. 13. The additional peak observed in the experimental data ~232 Hz is due to the modal response of the concrete base frame. Overall, the analytical predictions compare well with the experimental data.

3.2.3 Sound power

A discrete point intensity test in an "infinite baffle" condition was performed to obtain the sound power of the reference assembly for fifty-six 0.25 m × 0.25 m grids (shown in Fig. 14) in an anechoic chamber. The plate was excited using a TMS shaker (K2007E01) from the bottom side (not visible in Fig. 14), and the response was measured using a GRAS sound intensity probe, shown in Fig. 14 (microphones: 40AI). Foam was used to block the sound radiated from the bottom side of the plate to simulate "infinite baffle" conditions. The test details are presented in Table 3.

The ISO 9613 uncertainty test indicators[20] show that the measured test data gives a good estimation of the sound power of the test source. The surface pressure-intensity indicator (F2) and negative partial power indicator (F3) are well within the maximum allowable limit defined based on the pressure-residual index of the intensity probe and precision bias error[19]. In addition, the difference between F3 and F2 is within 3 dB for OTO bands higher than 100 Hz, which means that, below this OTO band, the results were affected by the extraneous noise[19]. The field non-uniformity indicator (F4) is well above the minimum requirement for OTO bands higher than 31.5 Hz, meaning that the measurement grid is adequate to calculate sound power within the allowable uncertainty[19].

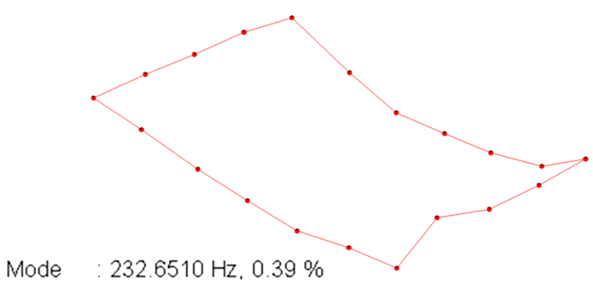

Fig. 7—A mode of the concrete base frame observed at ~232 Hz. This is the concrete mode observed in the 250 Hz OTO stabilization diagram.

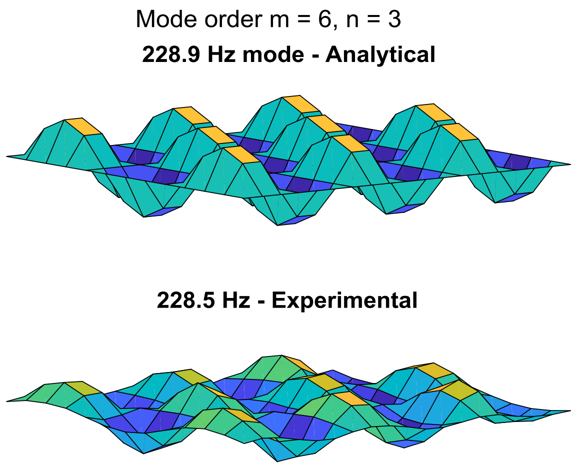

Fig. 8—228.9 Hz mode shows a good correlation between analytical and experimental data. All the other modes from 250 Hz OTO also show good correlation and are presented in Appendix A.

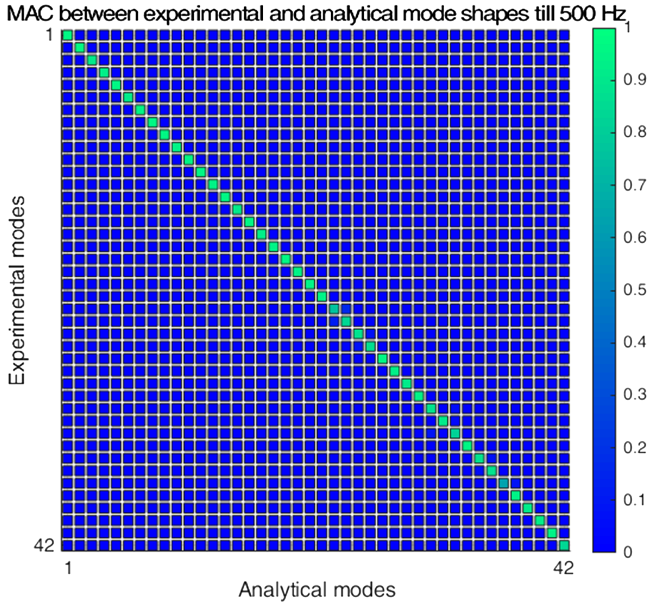

Fig. 9—MAC comparison shows correlation values greater than 0.9 between analytical and experimental data for the plate modes till 500 Hz.

Since the input signal was white Gaussian noise, the averaged force spectrum for all fifty-six grid points was slightly different from each other. To avoid complications, instead of using the measured response (Pa), frequency response functions (FRFs, output (Pa)/input (N)) were used.

The analytical and experimental results are compared with each other in Fig. 15 and the differences between the two are shown on the right-side axis. All the spectral values in this work are unweighted. In OTO bands lower than 125 Hz, the anechoic chamber is unable to block external noise from affecting the test results, based on its design. In frequencies ranging from 160 Hz to 400 Hz, the analytical predictions are within 1 to 2 dB of experimental data. For OTO bands higher than 400 Hz, the difference between the analytical and experimental data increases because of the fact that 0.25 m $\times$ 0.25 m grid spacing may not be fine enough to account for high-frequency variations in experimental sound power results using the sound intensity method. Some reasons for the differences in the analytical and experimental data are the following:

1. Sound radiated by the modes of the concrete base is not accounted in the analytical model.
2. Imperfect foam mounting at the bottom may allow some sound radiated from the bottom side to escape, which may lead to an increase in experimental readings.
3. Any variation in the shaker mounting location and stinger angle may result in differences in analytical and experimental data.

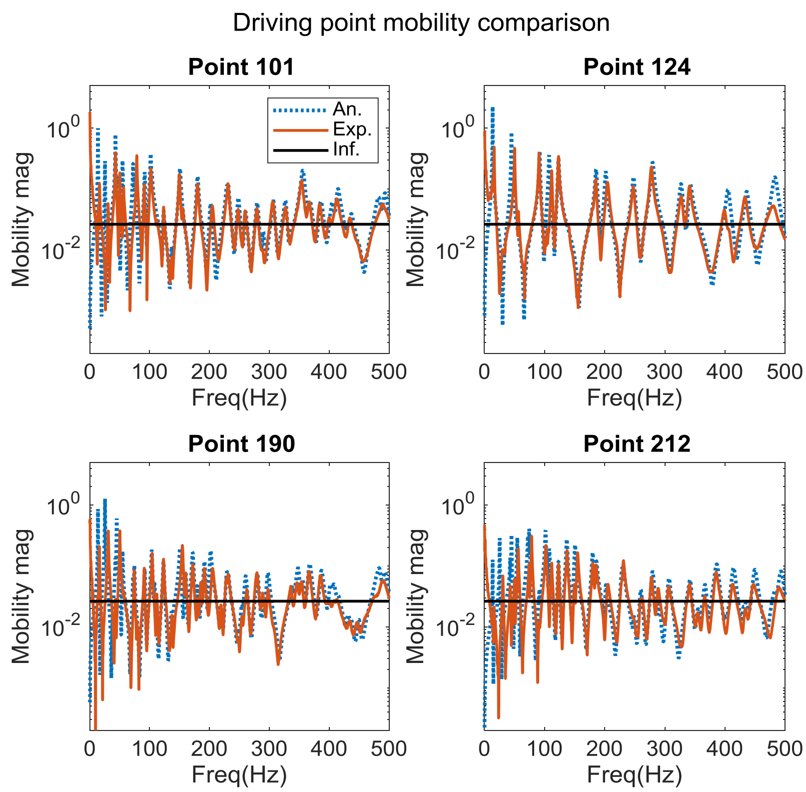

Fig. 10—Analytical and experimental driving point mobility for the frequencies 0 to 500 Hz. Analytical natural frequencies are within 1% to 2% of experimental natural frequencies on an average.

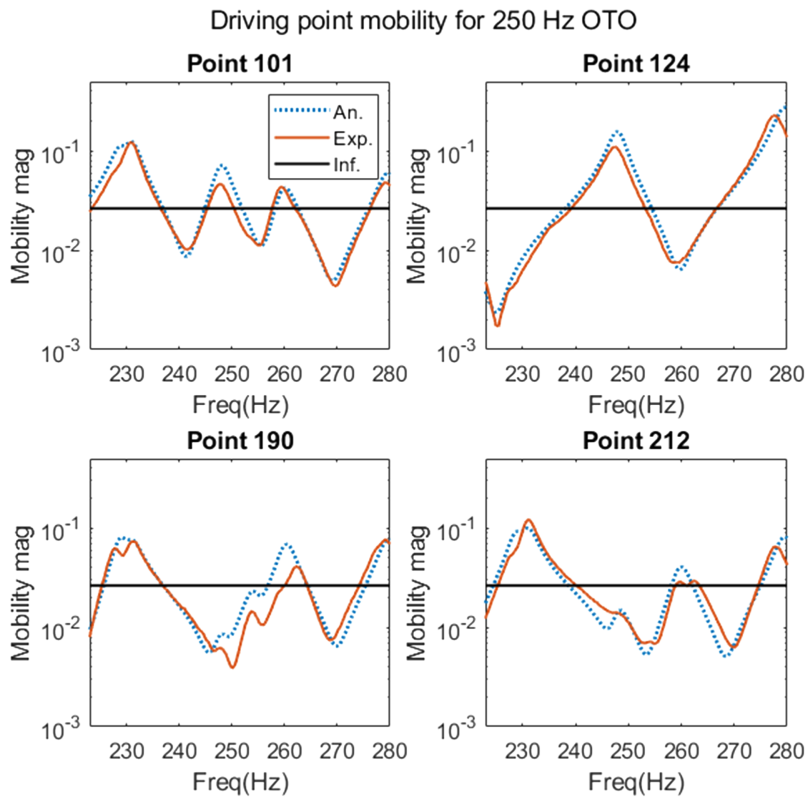

Fig. 11—Analytical and experimental driving point mobility for the 250 Hz OTO band. Analytical natural frequencies are within 1% to 2% of experimental natural frequencies on an average.

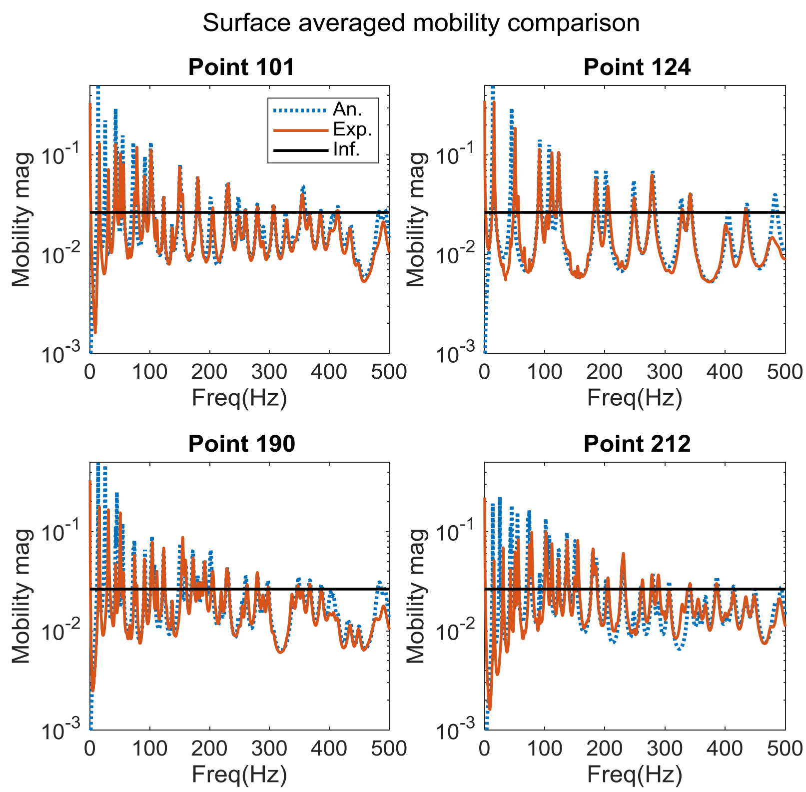

Fig. 12—Analytical and experimental surface averaged comparison from 0 Hz to 500 Hz. Analytical natural frequencies are within 1% to 2% of experimental natural frequencies on an average.

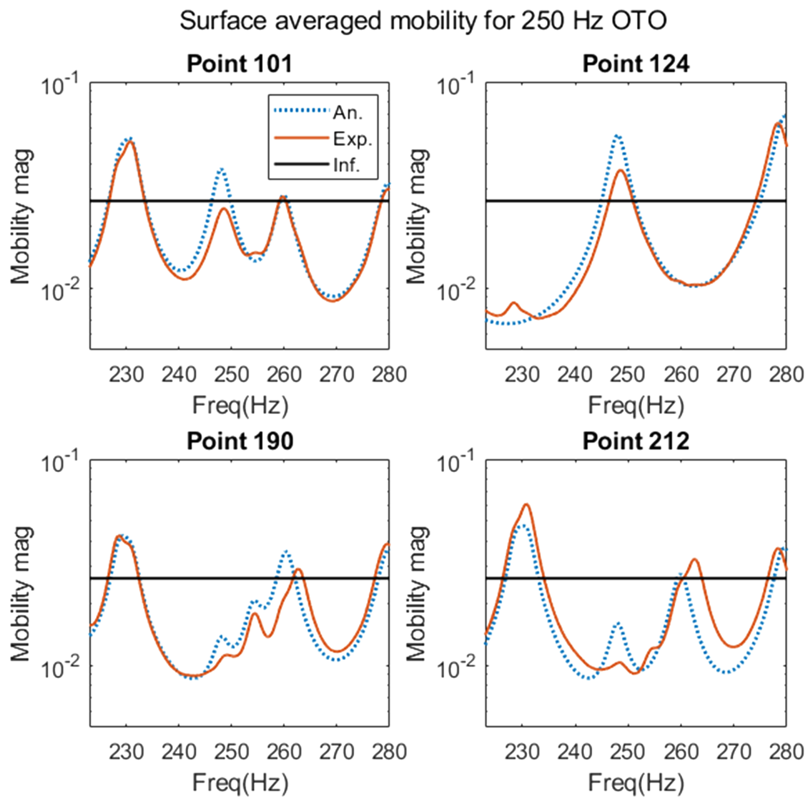

Fig. 13—Analytical and experimental surface averaged mobilities for 250 Hz OTO band. Analytical natural frequencies are within 1% to 2% of experimental natural frequencies on an average. The additional peak in the experimental response is due to the modal contribution of the concrete base frame.

Overall, the analytical predictions are close to the experimental data in mid-frequency bands. For this reference assembly, two sound power data sets are available—analytical and experimental, and these could be used to calculate the room contribution of a reverberation chamber.

3.3 Proof of Concept

With the sound power values of the reference assembly (analytical and experimental, both), the calibration factor between the known and the unknown plate can be calculated (using Eqn. 2) and used to obtain sound power of an

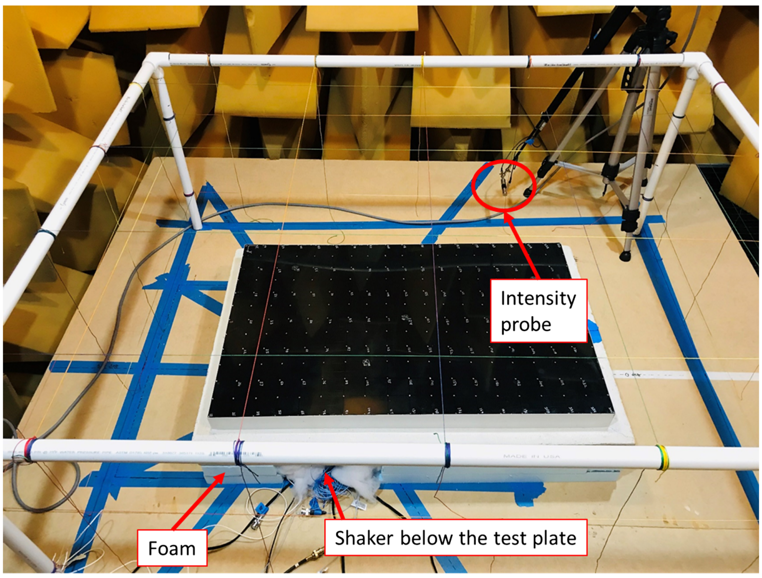

Fig. 14—Picture showing the sound intensity measurement grids, intensity probe, and foam. Input shaker cannot be seen in this picture.

Table 3—Test details for the intensity measurements of the reference plate.

Parameter	Value
Software used	Simcenter Testlab spectral testing
Frequency resolution (Δf)	0.25 Hz
Acquisition time	4 s
Bandwidth	2048 Hz
Number of averages	40
Window on all channels	Hanning
Shaker input signal	White Gaussian noise — 0.2 V RMS
Signal type	Burst random
Bandpass filter on input signal	10 Hz to 1024 Hz
Spacer for intensity probe	25 mm

unknown source (using Eq. 3). In full-scale laboratory settings, this unknown source would be the FC assembly, but for this study, a 30 in × 19 in × 0.13 in (762 mm × 482.6 mm × 3.3 mm) hardboard plate was used (shown in Fig. 16).

The sound power values for this assembly obtained through the proposed comparison technique were compared with baseline sound power values. These baseline values were obtained through a discrete point intensity test performed on the hardboard plate in infinite baffle conditions in the anechoic chamber. The boundary conditions of this plate were "free–free" (shown in Fig. 16). The test details were the same as tabulated in Table 3 with the exception that the shaker input signal level was reduced to 0.18 V to avoid disconnection of the shaker from the lightweight plate. The sound intensity measurement grid size was changed to 0.5 m × 0.25 m to reduce the total number of measurement points and total test time.

The reference assembly and the unknown, hardboard assembly were then tested in a reverberation chamber. The volume of this chamber was approximately 50 m^3, and based on the measured reverberation time, the Schroeder's cross-over frequency is approximately 350 Hz. Below 350 Hz, the reverberation chamber is non-diffuse, similar to the IIC test chambers. The data for the known and the unknown plates was measured in OTO bands as low as 80 Hz, well below the Schroeder cut-off frequency for the reverberation chamber. The measured SPL was averaged for two microphone locations (red circles in Fig. 17). The microphone locations were unchanged for both the tests.

Two sets of calibration factors were calculated using the analytical and experimental data for the reference plate. Using these calibration factors, two sets of sound power values were calculated for the hardboard assembly and compared with the baseline values, with the differences plotted on the right-side axis in Fig. 18. Once again the data below 125 Hz does not compare well as the exterior noise is affecting the anechoic intensity test. For 160 to 400 Hz OTO bands, the analytical CF method gives an error of 4 to 5 dB, and the experimental CF

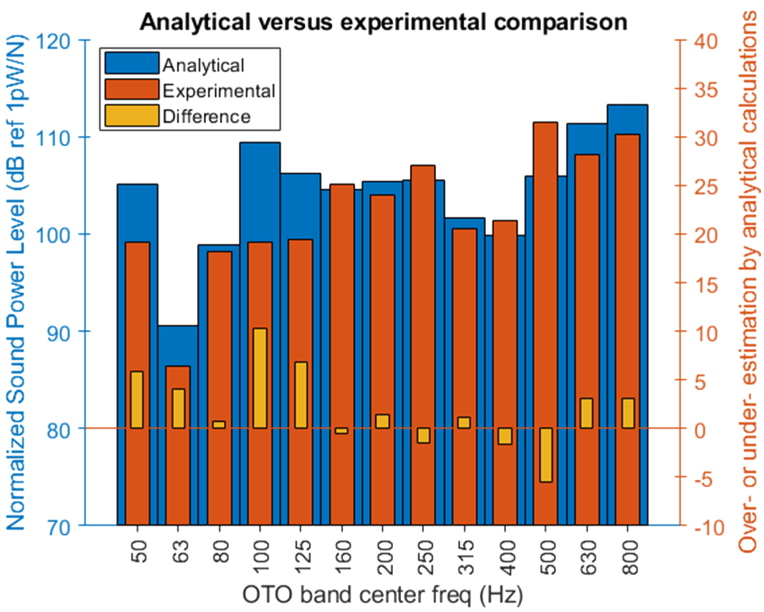

Fig. 15—Analytical data compared with experimental data and the difference is shown on the right-side axis. Note that the comparison in 160 to 400 Hz is expected to be better than the other OTO bands due to the restrictions of the anechoic test chamber and measurement grid size.

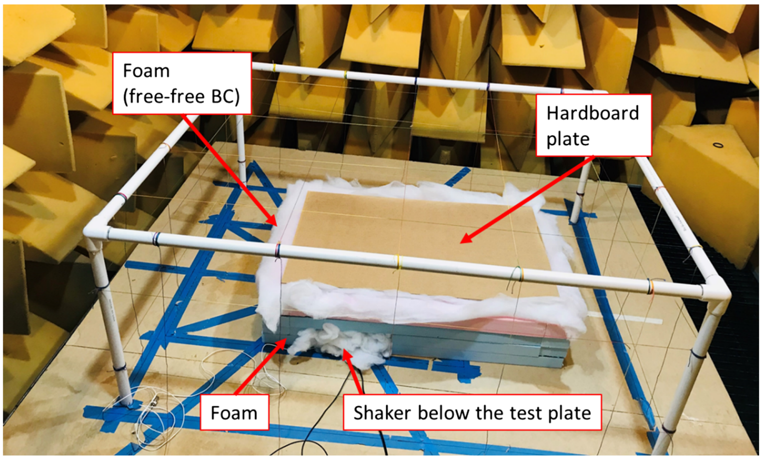

Fig. 16—Photograph of the sound intensity test that was performed for the unknown hardboard plate to obtain baseline sound power values.

method gives an error of 1 to 2 dB. Experimental CF makes a better prediction since the analytical calculations assume that the reference plate, the boundary conditions, etc. are perfect but the physical structure is not. Therefore, using experimental data instead of analytical results gives a better prediction for the hardboard assembly for mid-frequency OTO bands. For 500 to 800 Hz OTO band, the differences increase for both the methods since the intensity measurement grid size is not fine enough to capture variations at high frequencies.

For this small-scale assembly, the comparison method makes good sound power predictions except for the restrictions of the anechoic test chamber and the intensity measurement grid size. This method can be used to obtain reproducible sound-power measurements of the FC assemblies in laboratory tests and, therefore, can be used to improve the performance characterization of these assemblies.

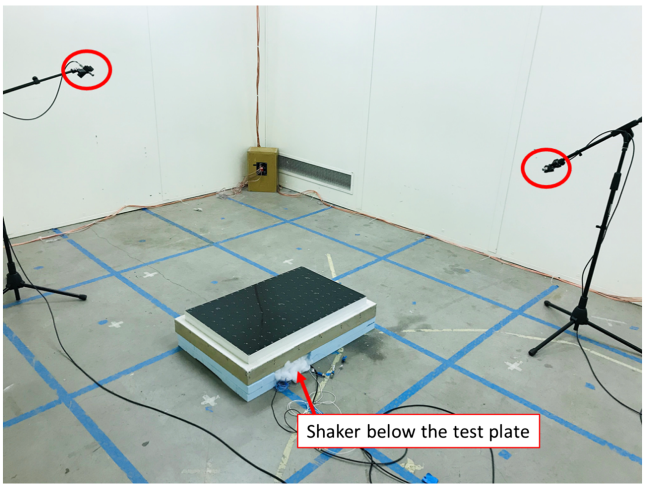

Fig. 17—Two microphone locations highlighted for the reverberation chamber test for the reference assembly and the new, hardboard assembly.

4 DISCUSSION

To implement the comparison method, IIC test laboratories can either perform analytical predictions on the reference assembly or obtain experimental sound power results. For the analytical method, the reference assembly should be uniform, homogeneous, and isotropic with controlled boundary conditions. For the experimental method, the reference assembly could have joints, welds, etc., as long as experimental sound power is obtained for OTO bands under consideration. Tests can be done either in the anechoic chamber (intensity measurement, hemi-anechoic measurement, etc.) or in the reverberation chamber (signal separation[21]). An important consideration is that the reference assembly is modally dense in the OTO bands to be studied. For example, a 12.5 ft × 10 ft × 0.03 ft (3.81 m × 3.05 m × 0.009 m) aluminum plate mounted with SS boundary conditions is modally dense in OTO bands 50 Hz and above[19].

This reference assembly with known boundary conditions should be mounted in the aperture in the IIC laboratories, and the input force should be given with the standard tapping machine (standard method gets rid of the limitations of imperfect shaker mounting observed in this study). The averaged SPL values should be used to compute the calibration factors of the room, and the reference assembly should be replaced with the actual FC assembly. The input force should be given using the tapping machine, and the measured SPL response should be used to calculate the sound power of the FC assembly.

The reference contour defined for the IIC rating uses SPL values, and using the same curve for sound power values would give erroneous results. Efforts would be

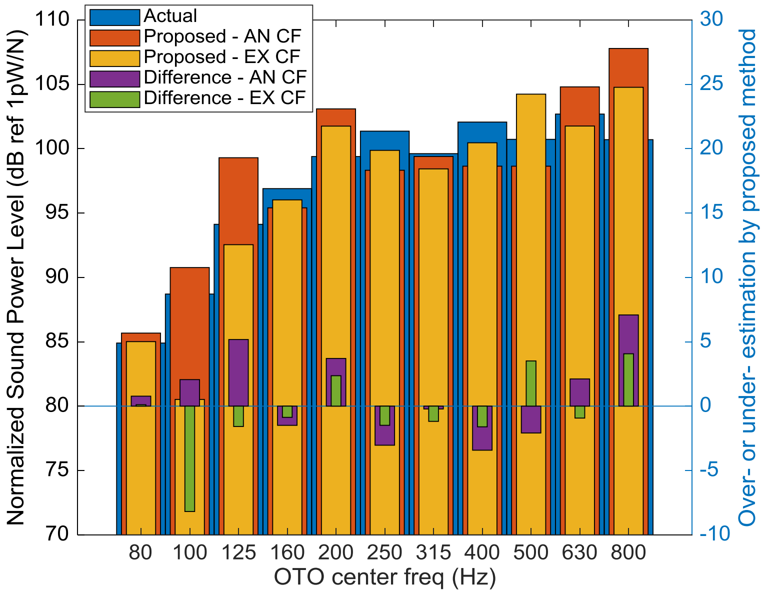

Fig. 18—Sound power values for the hardboard assembly using analytical and experimental CFs compared with baseline values. Note that comparison in 160 to 400 Hz OTO is expected to be better than the other OTO bands due to restrictions of the anechoic test chamber and measurement grid size. Experimental CFs make better predictions in the 160 to 400 Hz OTO bands as compared to analytical CFs.

required from the IIC test laboratories to develop a statistical sound power-based data set for various FC assemblies, which should be used to develop a new reference curve for IIC rating. This would require a long-term data set. Until that happens, an overall low-frequency sound power value (100 Hz to 315 Hz OTO bands) could be used to characterize FC assemblies, since this portion of the SPL reference curve defined in the standard is linearly weighted.

5 CONCLUSIONS AND FUTURE SCOPE

To truly characterize the FC assemblies, a source-based method such as sound power should be used instead of the existing source–path-based method such as sound pressure level. To reliably get to sound power from sound pressure measurements in a room, the proposed comparison method can be used. This comparison method can characterize the room contribution, thus establishing the relationship between sound power of the assembly and measured sound pressure level.

To characterize this room contribution, a reference assembly with known sound power was used in a reverberation room, and this room contribution was used to obtain the sound power of an unknown hardboard assembly. The sound power obtained using this method matched well with the baseline sound power level values obtained through discrete point intensity tests. The proof of concept of the proposed comparison method to test FC assemblies was shown for small-scale assemblies, and the analytical predictions for mode shapes, mobility, and sound power show good comparison with the experimental data for an ABS plastic plate with simply supported boundary conditions. A methodology has also been proposed for full-scale testing. Care must be taken during the full-scale testing since the radiation patterns of the assembly might be quite different.

The proposed method shows promising improvement over the existing method that suffers from limitations related to the non-diffuse low-frequency measurement field. The proposed method should not replace the existing IIC method but should act as a supplemental method for measuring and characterizing the performance of FC assemblies for low-frequency OTO bands. The standard tapping machine used for IIC tests could also be used for the proposed low-frequency measurement method.

This method enables a test engineer to make sound power measurements even in non-diffuse fields. A full-scale test needs to be done to verify whether the proposed method predicts reproducible sound power results. After this validation, it is recommended that this technique be added to the existing ASTM IIC measurement standard. This method also provides an improvement for some of the other ASTM test standards that make measurements in low-frequency OTO bands in reverberation rooms, such as ASTM E90[22], ASTM E336[23], and ASTM C423[24].

6 APPENDIX A. MODE SHAPE COMPARISON FOR 250 HZ OTO

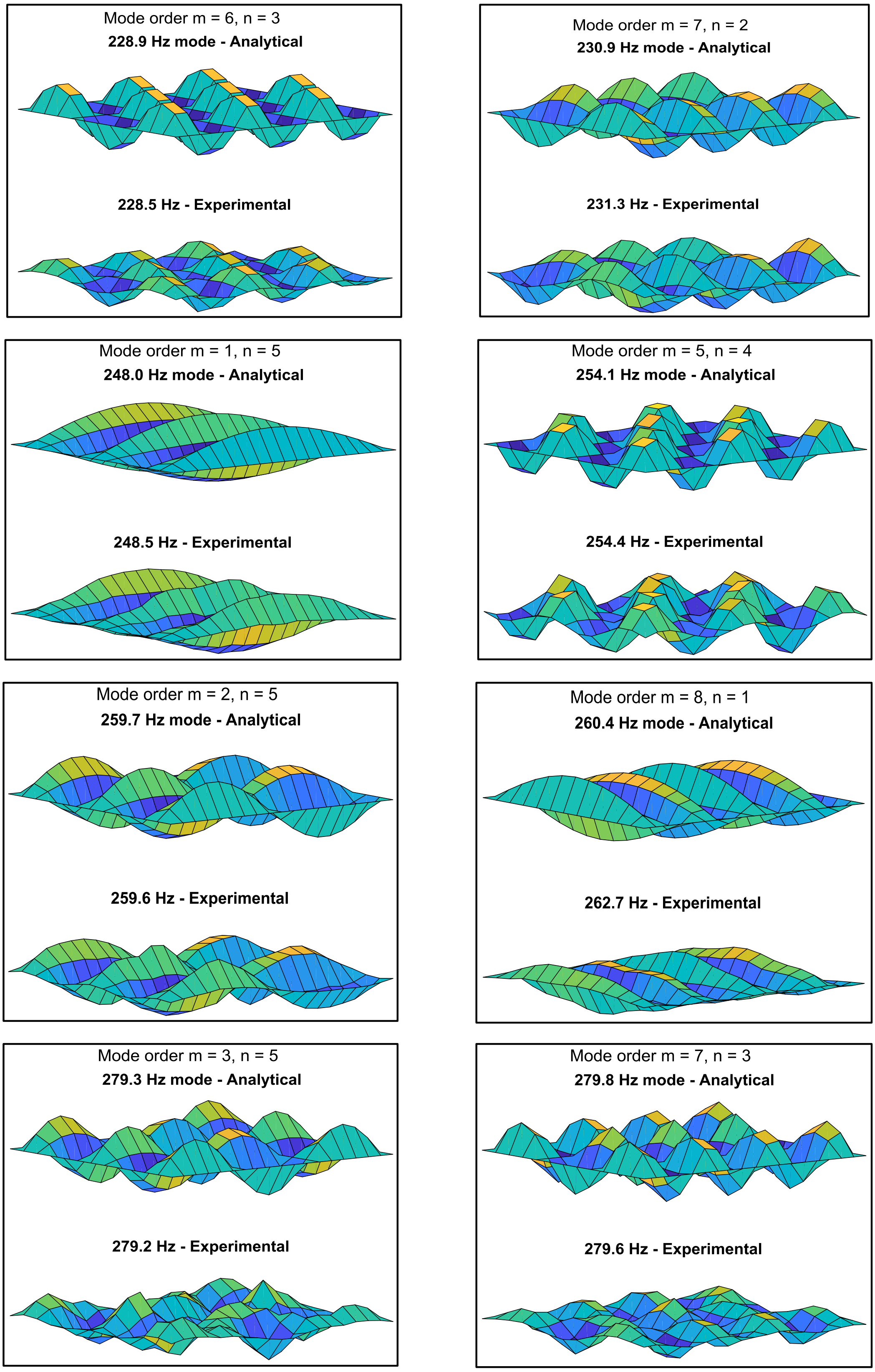

Appendix A—The analytical and experimental mode shapes show good comparison for the eight modes in 250 Hz OTO

7 ACKNOWLEDGMENTS

The authors would like to thank Mr. Carey Widder, President of GrassWorx LLC for funding the project and supporting the work throughout. The authors would also like to thank all the faculty and students associated with the Dynamic Systems Laboratory in the Mechanical Engineering — Engineering Mechanics department at Michigan Technological University.

8 REFERENCES

1. Standard Classification for Determination of Impact Insulation Class (IIC), ASTM_E989-06, (2012).
2. Acoustics — Rating of sound insulation in buildings and of building elements — Part 2: Impact sound insulation, ISO_717-2, (2013).
3. Standard Test Method for Laboratory Measurement of Impact Sound Transmission Through Floor-Ceiling Assemblies Using the Tapping Machine, ASTM_E492-09, (2016).
4. F. Ljunggren, C. Simmons, and K. Hagberg, "Correlation between sound insulation and occupants' perception–Proposal of alternative single number rating of impact sound", *Applied Acoustics*, **85**, 57–68, (2014).
5. W.E. Blazier Jr. and R.B. DuPree, "Investigation of low-frequency footfall noise in wood-frame, multifamily building construction", *J. Acoust. Soc. Am.*, **96**(3), 1521–1532 (1994).
6. T. Mariner and H.W.W. Hehmann, "Impact-noise rating of various floors", *J. Acoust. Soc. Am.*, **41**(1), 206–214 (1967).
7. J.R. Nordstedt, "Comparison between different methods for impact testing of floors", *J. Acoust. Soc. Am.*, **65**(2), 418–424 (1979).
8. D. Olynyk and T.D. Northwood, "Subjective judgments of foot-step-noise transmission through floors", *J. Acoust. Soc. Am.*, **38**(6), 1035–1039 (1965).
9. R. Öqvist, F. Ljunggren, and R. Johnsson, "Walking sound annoyance vs. impact sound insulation from 20 Hz", *Applied Acoustics*, **135**, 1–7, (2018).
10. J.J. LoVerde and D.W. Dong, "A dual-rating method for evaluating impact noise isolation of floor-ceiling assemblies", *J. Acoust. Soc. Am.*, **141**(1), 428–440 (2017).
11. A. Barnard, S. Girdhar, M. Penhale, and C. Widder, "Evaluation of receiving room diffusivity and the effect on low frequency impact insulation class", Proc. Inter-noise and Noise-con Congress and Conference Proceedings, Chicago, Illinois, USA, Vol. **258**, pp. 5695-5706, (2018).
12. Laboratory Measurement of the Airborne Sound Barrier Performance of Flat Materials and Assemblies, SAE_J1400, (2010).
13. S.A. Hambric, S.H. Sung, and D.J. Nefske, "*Engineering Vibroacoustic Analysis: Methods and Applications*", John Wiley & Sons, (2016).
14. C.E. Wallace, "Radiation resistance of a rectangular panel", *J. Acoust. Soc. Am.*, **51**(3B), 946–952 (1972).
15. G. Squicciarini, D.J. Thompson, and R. Corradi, "The effect of different combinations of boundary conditions on the average radiation efficiency of rectangular plates", *J. Sound Vib.*, **333**(17), 3931–3948 (2014).
16. F.J. Fahy, "*Sound and structural vibration: radiation, transmission and response*", Academic Press, (1985).
17. F.J. Fahy, "Measurement of acoustic intensity using the cross-spectral density of two microphone signals", *J. Acoust. Soc. Am.*, **62**(4), 1057–1059 (1977).
18. O. Robin, J.-D. Chazot, R. Boulandet, M. Michau, A. Berry, and N. Atalla, "A plane and thin panel with representative simply supported boundary conditions for laboratory vibroacoustic tests", *Acta Acust. united Ac.*, **102**(1), 170–182 (2016).
19. S. Girdhar, "Improved low-frequency impact insulation class measurements based on comparison techniques," in Open Access Master's Report. Michigan Technological University, Houghton, MI, 49931, 2019.
20. Acoustics—Determination of sound power levels of noise sources using sound intensity: Part 1, ISO_9614-1, (1993).
21. A. Barnard, S. Hambric, J. Maynard, "Underwater measurement of sound power and directivity using Supersonic Intensity in Reverberant Environments," *J. Sound and Vib.,* **331**, 3931–3944, (2012).
22. Standard Test Method for Laboratory Measurement of Airborne Sound Transmission Loss of Building Partitions and Elements, ASTM_E90-09, (2016).
23. Standard Test Method for Measurement of Airborne Sound Attenuation between Rooms in Buildings, ASTM_E336-17, (2019).
24. Standard Test Method for Sound Absorption and Sound Absorption Coefficients by the Reverberation Room Method, ASTM_C423-17, (2017).